

Functionalization of Carbon Nanotubes with Vaska's Complex: A Theoretical Approach

Francesco Mercuri* and Antonio Sgamellotti

ISTM-CNR and Dipartimento di Chimica, Università di Perugia, I-06123 Perugia, Italy

Received: February 13, 2006; In Final Form: February 21, 2006

The functionalization of single-walled carbon nanotubes (CNTs) with Vaska's complex $\text{trans-Ir(CO)Br(PPh}_3)_2$ has been investigated by means of hybrid quantum mechanics/molecular mechanics (QM/MM) calculations. The formation of a stable adduct has been experimentally evidenced by Wong et al. (*Nano Lett.* **2002**, 2, 49), but microscopical details on the metal–nanotube interaction are still unclear. Our calculations show a low propensity to η^2 coordination of Vaska's complex with the perfect hexagonal network of CNTs. Rather, a stronger interaction takes place when the transition metal center coordinates to carbon atoms belonging to pentagonal rings, as in topological defects or end-caps.

Introduction

Carbon nanotubes (CNTs)¹ have been the focus of intense research, in the past decade, as a consequence of their promising employment in the field of nanotechnology. However, a number of applications involve chemical modifications of the sidewall in order to achieve better solubility and processability, changes in the electronic and/or mechanical properties, and, in general, tunable attributes of the functionalized adduct.^{2,3} Despite its importance, the chemistry of CNTs is still in its early stages and the functionalization of the sidewall is currently being investigated by several research groups.⁴ Indeed, the establishment of a “well-defined” chemistry of CNTs is a necessary condition for several of their further applications. In particular, new directions for the functionalization of CNTs have been opened by the extension of transition metal chemistry to the interaction with the sidewall, as recently demonstrated by Wong et al. in the case of iridium, rhodium, and osmium complexes.^{5,6} However, due to the complexity of the experimental setup and intrinsic limitations of measurement procedures, many aspects concerning the microscopic nature of the functionalization process remain, to a large extent, unexplored. Hence, theoretical investigations can shed light at a microscopic level of detail, revealing particularities such as coordination modes, the stability and structure of the adducts, and their electronic properties. As a consequence, a few papers appeared recently concerning theoretical calculations on CNTs functionalized by transition metal compounds, such as Cr(CO)_3 ,^{7,8} and OsO_4 .⁹ Moreover, recent investigations^{10,11} point out the role played by topological and structural defects on the CNT sidewall in determining their properties and, consequently, their chemistry. Thus, defects on the hexagonal carbon atom network can be viewed as likely interaction sites, opening the way toward new functionalization schemes, whereas the reaction routes usually considered involve highly reactive functional groups.⁴

In this work, the interaction between single-walled CNTs and Vaska's complex¹² is studied through density functional theory (DFT) calculations, thus providing a case study of CNT functionalization with electron-rich transition metal complexes. The formation of stable adducts has been experimentally shown by Banerjee and Wong.⁵ In calculations, finite-length models of a (9,0) CNT, terminated with hydrogens or capped with two half- C_{60} moieties (see Figure 1), were considered. Moreover,

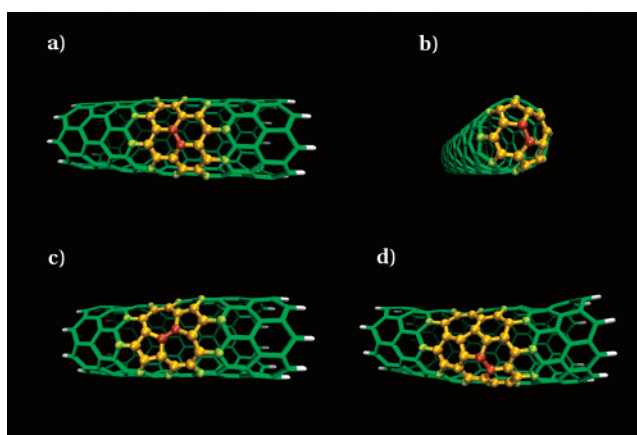


Figure 1. Models of (9,0) CNTs used in calculations. Atoms included in the QM part are shown in the ball-and-stick representation (yellow), link atoms (hydrogens) in light green, and carbon atoms coordinating to iridium in dark orange: (a) defect-free sidewall; (b) capped end; (c) SW (pentagon–heptagon pair) defect; (d) single pentagon–heptagon defect originating from the displacement of a SW pair.

the effects due to the presence of topological defects on CNTs on the functionalization process were taken into account by models in which structural changes of the perfect hexagonal network of the sidewall were introduced.

Computational Details

Calculations were performed by adopting a hybrid quantum mechanics/molecular mechanics (QM/MM) approach¹³ as implemented in the ADF program package.¹⁴ For the MM part, the Tripos force field¹⁵ was used, whereas DFT was adopted for the description of the QM part. DFT calculations were carried out within Becke¹⁶ and Perdew¹⁷ corrections to the local density approximation. Vaska's complex and a portion of the CNT sidewall, ranging from 16 to 24 carbon atoms, were included in the QM part. The QM/MM partitioning for the CNTs is shown in Figure 1. A double- ζ -quality basis set was used for all atoms in the QM part, with the exception of the iridium atom, where a triple- ζ -quality basis set was used. A frozen core approximation was used for inner shells of atoms, and relativistic effects were included through the scalar ZORA formalism.¹⁸ The adopted QM treatment for the metal complex gives in

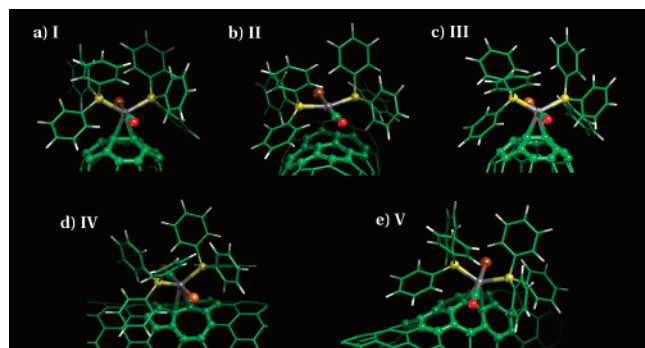


Figure 2. Optimized structures of complexes **I–V** (for clarity, only the relevant part of the models is shown). Atoms included in the QM part are shown in the ball-and-stick representation.

general a good description of the metal–ligand interaction,¹⁹ whereas the MM parametrization is known to give good results for π – π interactions²⁰ which might occur between the phenylic ligands and the nanotube sidewall. The hybrid QM/MM formalism has been successfully applied in recent theoretical investigations on the functionalization of CNTs.^{21,22} Indeed, the locality of chemical interactions allows an accurate description of the functionalization process even though only small portions of the sidewall are included in calculations.^{21,23} Binding energies (BEs) were evaluated as the energy of the adduct minus the sum of the energies of the isolated metal complex and CNT. Reported BEs only take into account the QM contribution. Corrections to the basis set superposition error (BSSE) were introduced according to the counterpoise scheme.²⁴ Full geometry optimizations were carried out for all systems without any symmetry constraint.

Results and Discussion

A validation of our computational approach has been carried out by analyzing the interaction of Vaska's complex *trans*-Ir(CO)Cl(PPh₃)₂ with C₆₀, which gives rise to an adduct whose structure is experimentally well-known.²⁵ Similar to the case of coordination with tetracyanoethylene,²⁶ upon coordination, the iridium center loses the square-planar conformation with a distortion of the P–Ir–P angle up to 113° (Figure 2a). As shown in Table 1 (complex **I**), computed geometrical parameters are in good agreement with the experimental structure and the QM/MM approach allows an adequate description of both the metal center coordination and the aromatic–aromatic interactions (see the Ph–C₆₀ distance) at a relatively low computational cost.

In experimental studies on the functionalization of CNTs with Vaska's complex *trans*-Ir(CO)Br(PPh₃)₂,^{4,5} an η^2 coordination of the metal center with the sidewall is postulated, analogously to the case of fullerene. However, calculations performed on the coordination of Vaska's complex coordinated to the sidewall of a (9,0) CNT, in different configurations, did not lead to strong evidence of a relevant interaction between the iridium center and the carbon atom surface. In all of the examined cases, we were not able to find a stable bound adduct between the sidewall and Vaska's complex. Rather, a weakly bound complex is formed, in which a π – π stacking interaction between the phenylic rings and the CNT sidewall takes place. In the most relevant case (complex **II** in Table 1, Figure 2b, and Figure 1a), the small, positive BE for the quantum part indicates a slightly repulsive interaction between the iridium complex and the sidewall, partially compensated by the aromatic π – π stacking. This effect was confirmed by the geometry optimization of the complex *trans*-Ir(CO)Br(PH₃)₂ on the CNT sidewall in the same coordination mode, which provided a very similar structure for the weakly bound adduct, with slightly longer Ir–C distances (3.598 and 3.573 Å, respectively). As a result, the P–Ir–P angle is well beyond the typical value for the interaction of Vaska's complex with a carbon–carbon double bond²⁶ or with the 6–6 ring fusion in C₆₀. The lack of coordination can be related to the reduced reactivity of C–C bonds in nanotube sidewalls with respect to ordinary alkenes and fullerenes,³ as will be discussed later, and to the reduced number of possible coordination modes, due to the sterical hindrance of bulky groups of Vaska's complex.

Looking for suitable coordination schemes between Vaska's complex and CNTs, another attempt was made by modeling the interaction with the nanotube's end-cap. Indeed, the enhanced reactivity of end-caps with respect to the sidewall has already been addressed in theoretical studies on the functionalization of CNTs with different species.^{3,27} In this case, the metal center was η^2 -coordinated to the bond between two carbon atoms on the end-cap at a 6–6 ring fusion (see Figure 1b), thus modeling the interaction with a pyraclyenic unit of the CNT tip. As expected, optimized geometrical parameters and the binding energy (complex **III** in Table 1 and Figure 2c) suggest the formation of a stable adduct (–126 kJ mol^{–1}), in a configuration very similar to the case of the coordination of Vaska's complex with C₆₀. Indeed, the chemical picture of a transition metal complex coordinating on a nanotube end-cap resembles the situation arising for the interaction with C₆₀: the Ir–C distances for Vaska's complex coordinated to the nanotube

TABLE 1: Geometrical Parameters for the Optimized Structures I–V (Distances in Angstroms, Angles in Degrees)

		I	II	III	IV	V
	C ₆₀ ^a (exptl)	C ₆₀ (theor)	sidewall	end-cap	SW defect	5–7 pair
Ir–C _{NNT}	2.189	2.218/2.212	3.393/3.417	2.222/2.217	2.483/2.460	2.356/2.506
Ir–P	2.384	2.359/2.357	2.309/2.322	2.363/2.395	2.343/2.339	2.321/2.340
Ir–C _{CO}	1.923	1.850	1.832	1.848	1.852	1.847
Ir–X ^b	2.402	2.436	2.394	2.435	2.428	2.416
C–O		1.164	1.173	1.166	1.166	1.166
C–Ir–C	41.0	40.7	24.1	39.9	44.6	34.3
P–Ir–P	113.3	121.9	160.6	124.9	123.1	130.5
Ph–C ₆₀ ^c	3.304	3.358				
Pyram. angle ^d	16.1/15.6	15.5/15.5	5.2/5.3	16.2/16.2	5.4/5.7	14.9/8.5
BE(QM) ^e		–124.2	13.5	–125.8	–35.5	–28.5
π^f		–7.09	–7.08	–7.06	–7.09	–7.77
π^{*f}		–3.15	–2.46	–2.64	–3.70	–3.84
ΔE^f		3.94	4.62	4.42	3.39	3.93

^a Reference 25. ^b X = Cl (complex **I**) or Br (complexes **II–V**). ^c Average distance (in angstroms) between the C₆₀ surface and the center of the two closest phenylic rings of Vaska's complex. ^d Pyramidalization angle defined as in ref 3. ^e Binding energies in kilojoules per mole (see text). ^f Energy of the coordinating C–C occupied π and unoccupied π^* orbitals and energy gap (ΔE) in electronvolts.

end-cap result (2.222 and 2.216 Å, respectively) in a close agreement with the case of coordination with C₆₀ (2.218 and 2.213 Å). However, sterical hindrance could limit the possibilities of interaction with the end-cap to CNTs with diameters comparable to that of a C₆₀ unit. Furthermore, since the end-caps are only a limited portion of the nanotube surface available for the coordination with the metal center, the functionalization at the terminating tip could not completely explain the experimental evidence of a remarkable interaction between the two species.

Hence, the possibility of stronger interactions between defective sites of CNT sidewalls and Vaska's complex was analyzed. We first considered the case of a topological Stone–Wales (SW) defect,²⁸ consisting of two adjacent pairs of pentagonal and heptagonal rings on the perfect hexagonal network of a nanotube sidewall, as shown in Figure 1c. SW defects represent a common feature of the sidewall, even after energetic curing processes and have been recently advocated as responsible of the strong observed chemisorption of small molecules on CNTs.^{11,29} In the case of a SW defect, calculations performed on the complex shown in Figure 2d, in which the metal center is η^2 -coordinated with the C–C bond, indicate a remarkable interaction between Vaska's complex and the defected surface of a (9,0) CNT sidewall (complex **IV** in Table 1). A BE of -36 kJ mol^{-1} was found for a particular orientation of the SW defect with respect to the CNT axis (see Figure 2d), whereas other configurations (e.g., with the coordinating C–C bond parallel or orthogonal to the CNT axis) lead to lower interaction energies. We also considered the displacement of the pentagonal–heptagonal ring pair on two different zones of the nanotube sidewall, a process commonly induced by mechanical strain³⁰ (see Figure 1d). Geometry optimization was performed on the complex shown in Figure 2e, with Vaska's complex η^2 -coordinated with two carbon atoms belonging to a pentagonal and a hexagonal ring, respectively, which, in turn, originate from the displacement of a SW defect. We can consider this configuration as an intermediate case between the η^2 interaction with pyracenylic units, as in C₆₀ or nanotube end-caps, and the interaction with pyrenic units, as in the case of the defect-free nanotube sidewall. Computed geometries and the interaction energy, shown in the last column of Table 1 (complex **V**), evidence the formation of a stable adduct between Vaska's complex and the defective site in an η^2 coordination. However, the coordination mode is less symmetric than that in the case of the SW defect, with a shorter Ir–C distance for the carbon atom belonging to the pentagonal ring. The formation of a stable bound structure was further confirmed by frequency calculations performed on the optimized geometry, in which only positive frequencies were found. The BE (-29 kJ mol^{-1}) also indicates a slightly reduced interaction with the SW defect case, due to the presence of only one pentagonal ring at the coordination site.

The observed energies and structures for the different adducts can be rationalized in terms of pyramidalization angle and orbitalic structure at the coordination site.³ As shown in Table 1, the increase in the pyramidalization angle, due to the presence of defects, leads to a higher propensity to reaction. As a consequence, an enhancement of the reactivity can be expected for CNTs of smaller diameters. Moreover, the electronic structure of the adduct can be analyzed by applying the Dewar–Chatt–Duncanson model for the interaction between an electron-rich transition metal complex and a π system.³¹ In this case, the main interactions are the σ donation, from the occupied molecular orbitals (MOs) of the ligand, and the π back-donation

from occupied d orbitals of the metal fragment to the empty π^* orbitals of the alkenic moiety. Recent DFT calculations⁸ indicate that the presence of pentagonal rings, as in fullerenes, influences the relative energy of frontier orbitals of the organic fragment, thus enhancing the affinity of the system for electron-rich metal complexes, with respect to fragments constituted of six-term rings. In particular, the reactivity of the coordinating C–C bond can be related to the energy of occupied π and empty π^* orbitals. Thus, the energy gap between the two corresponding mono-electronic orbitals could account for different reactivity propensities. As shown in Table 1, the trend observed for bent polycyclic aromatic hydrocarbon models⁸ is confirmed by our calculations which indicate a larger binding energy for CNTs with a smaller gap between the π occupied and π^* empty orbitals and, in particular, with a lower π^* orbital energy.³² Thus, when the metal center coordinates with pyrenic units, as in the case of the defect-free sidewall, the high energy of the unoccupied π^* orbital prevents efficient π back-donation. On the other hand, coordination with pyracenylic units or, in general, an η^2 coordination with one or two carbon atoms belonging to pentagonal rings can give rise to stable complexes, due to a more favorable MO structure for interaction with the metal center. The overall binding energy can then be considered as a result of the interplay between structural factors, as indicated by the pyramidalization angle, and the subsequent modification of the electronic structure in the region of frontier orbitals.

Conclusions

In conclusion, possible interaction modes for the interaction between unoxidized CNTs and Vaska's complex were analyzed by means of theoretical calculations, thus providing a model for the functionalization with electron-rich transition metal compounds. We were not able to find a stable bound adduct between Vaska's complex and the perfect hexagonal network of a (9,0) CNT, thus suggesting that the sidewall is relatively inert to an attack from Vaska's complex. However, nanotube end-caps or defective sites on the sidewall show a higher propensity to coordination with the inorganic fragment, indicating such sites as more suitable coordination centers for an η^2 bonding, similarly to the case of C₆₀. Hence, a stable adduct is more likely to be formed when at least one of the coordinating carbon atoms belongs to a pentagonal ring. This picture extends the possibility of functionalizing CNTs with transition metal complexes and confirms the role of topological defects concerning the reactivity of the sidewall.

Supporting Information Available: 3D rotatable images of the optimized structures **I–V** in both xyz and VRML2.0 formats. This material is available free of charge via the Internet at <http://pubs.acs.org>.

References and Notes

- (1) Iijima, S.; Ichihashi, T. *Nature* **1992**, *363*, 603.
- (2) (a) *Carbon Nanotubes: Synthesis, Structure, Properties and Applications*; Dresselhaus, M. S.; Dresselhaus, G.; Avouris, P., Eds.; Springer: Berlin, Germany, 2001. (b) Zhao, J.; Chen, Z.; Zhou, Z.; Park, H.; Schleyer, P. v. R.; Lu, J. P. *ChemPhysChem* **2005**, *6*, 598. (c) Dyke, C. A.; Tour, J. M. *Chem.–Eur. J.* **2004**, *10*, 813. (d) Hirsch, A. *Angew. Chem., Int. Ed.* **2002**, *41*, 1853. (e) Chen, J.; Hamon, M. A.; Hu, H.; Chen, Y. S.; Rao, A. M.; Eklund, P. C.; Haddon, R. C. *Science* **1998**, *282*, 95.
- (3) Niyogi, S.; Hamon, M. A.; Hu, H.; Zhao, B.; Bhowmik, P.; Sen, R.; Itkis, M. E.; Haddon, R. C. *Acc. Chem. Res.* **2002**, *35*, 1105.
- (4) See, for instance, the following review: Banerjee, S.; Hemraj-Benny, T.; Wong, S. S. *Adv. Mater.* **2005**, *17*, 17 and references therein.
- (5) Banerjee, S.; Wong, S. S. *Nano Lett.* **2002**, *2*, 49.
- (6) (a) Banerjee, S.; Wong, S. S. *J. Am. Chem. Soc.* **2002**, *124*, 8940. (b) Banerjee, S.; Wong, S. S. *J. Am. Chem. Soc.* **2004**, *126*, 2073.

- (7) (a) Nunzi, F.; Mercuri, F.; De Angelis, F.; Sgamellotti, A.; Giannozzi, P. *J. Phys. Chem. B* **2004**, *108*, 5243. (b) Nunzi, F.; Mercuri, F.; Re, N.; Sgamellotti, A. *Mol. Phys.* **2003**, *101*, 2047.
- (8) Nunzi, F.; Mercuri, F.; Re, N.; Sgamellotti, A. *J. Phys. Chem. B* **2002**, *106*, 10622.
- (9) Lu, X.; Tian, F.; Feng, Y. B.; Xu, X.; Wang, N. Q.; Zhang, Q. N. *Nano Lett.* **2002**, *2*, 1325.
- (10) (a) Lu, X.; Chen, Z. F.; Schleyer, P. v. R. *J. Am. Chem. Soc.* **2005**, *127*, 20. (b) Charlier, J.-C. *Acc. Chem. Res.* **2002**, *35*, 1063. (c) Hashimoto, A.; Suenaga, K.; Gloter, A.; Urita, K.; Iijima, S. *Nature* **2004**, *430*, 870.
- (11) (a) Mercuri, F.; Sgamellotti, A.; Valentini, L.; Armentano, I.; Kenny, J. M. *J. Phys. Chem. B* **2005**, *109*, 13175. (b) Valentini, L.; Mercuri, F.; Armentano, I.; Cantalini, C.; Picozzi, S.; Lozzi, L.; Santucci, S.; Sgamellotti, A.; Kenny, J. M. *Chem. Phys. Lett.* **2004**, *384*, 356. (c) Bettinger, H. F. *J. Phys. Chem. B* **2005**, *109*, 6922.
- (12) Vaska, L. *Science* **1963**, *140*, 809.
- (13) (a) Woo, T. K.; Cavallo, L.; Ziegler, T. *Theor. Chem. Acc.* **1998**, *100*, 307. (b) Maseras, F.; Morokuma, K. *J. Comput. Chem.* **1995**, *16*, 1170.
- (14) ADF2004.01, SCM, Theoretical Chemistry, Vrije Universiteit, Amsterdam, The Netherlands, <http://www.scm.com>.
- (15) Clark, M.; Cramer, R. D., III; Van Opdenbosch, N. *J. Comput. Chem.* **1989**, *10*, 982.
- (16) Becke, A. D. *Phys. Rev. A* **1988**, *38*, 3098.
- (17) Perdew, J. P. *Phys. Rev. B* **1986**, *33*, 8822.
- (18) (a) van Lenthe, E.; Ehlers, A. E.; Baerends, E. J. *J. Chem. Phys.* **1999**, *110*, 8943. (b) van Lenthe, E.; Baerends, E. J.; Snijders, J. G. *J. Chem. Phys.* **1993**, *99*, 4597. (c) van Lenthe, E.; Baerends, E. J.; Snijders, J. G. *J. Chem. Phys.* **1994**, *101*, 9783. (d) van Lenthe, E.; Snijders, J. G.; Baerends, E. J. *J. Chem. Phys.* **1996**, *105*, 6505. (e) van Lenthe, E.; van Leeuwen, R.; Baerends, E. J.; Snijders, J. G. *Int. J. Quantum Chem.* **1996**, *57*, 281.
- (19) (a) Deng, L. Q.; Woo, T. K.; Cavallo, L.; Margl, P. M.; Ziegler, T. *J. Am. Chem. Soc.* **1997**, *119*, 6177. (b) Woo, T. K.; Margl, P. M.; Blochl, P. E.; Ziegler, T. *J. Phys. Chem. B* **1997**, *101*, 7877. (c) Mercuri, F.; Sgamellotti, A.; Re, N. *Theor. Chem. Acc.* **2002**, *108*, 46.
- (20) Magistrato, A.; Pregosin, P. S.; Albinati, A.; Rothlisberger, U. *Organometallics* **2001**, *20*, 4178.
- (21) Bauschlicher, C. W. *Chem. Phys. Lett.* **2000**, *322*, 237.
- (22) (a) Kar, T.; Akdim, B.; Duan, X. F.; Pachter, R. *Chem. Phys. Lett.* **2004**, *392*, 176. (b) Basiuk, E. V.; Basiuk, V. A.; Banuelos, J. G.; Saniger-Blesa, J. M.; Pokrovskiy, V. A.; Gromovoy, T. Y.; Mischanchuk, A. V.; Mischanchuk, B. G. *J. Phys. Chem. B* **2002**, *106*, 1588.
- (23) Bauschlicher, C. W. *Nano Lett.* **2001**, *1*, 223.
- (24) Boys, S. F.; Bernardi, F. *Mol. Phys.* **1970**, *19*, 553.
- (25) Balch, A. L.; Catalano, V. J.; Lee, J. W. *Inorg. Chem.* **1991**, *30*, 3980.
- (26) McGinnety, J. A.; Ibers, J. A. *Chem. Commun.* **1968**, *5*, 235.
- (27) Basiuk, E. V.; Monroy-Pelaez, M.; Puente-Lee, I.; Basiuk, V. A. *Nano Lett.* **2004**, *4*, 863.
- (28) Stone, A. J.; Wales, D. J. *Chem. Phys. Lett.* **1986**, *128*, 501.
- (29) Chakrapani, N.; Zhang, Y. M.; Nayak, S. K.; Moore, J. A.; Carroll, D. L.; Choi, Y. Y.; Ajayan, P. M. *J. Phys. Chem. B* **2003**, *107*, 9308.
- (30) Nardelli, M. B.; Yakobson, B. I.; Bernholc, J. *Phys. Rev. B* **1998**, *57*, R4277.
- (31) (a) Dewar, M. J. S. *Bull. Soc. Chim. Fr.* **1951**, *18*, C71. (b) Chatt, J.; Duncanson, L. A. *J. Am. Chem. Soc.* **1953**, *75*, 9.
- (32) When comparing the energy of π and π^* orbitals, the different size of the QM part, included in calculations, must be taken into account. Thus, smaller QM parts could result in slightly higher computed energy gaps.